

OPEN

# Strain-induced switching of heat current direction generated by magneto-thermoelectric effects

Shinya Ota<sup>1,2</sup>, Ken-ichi Uchida<sup>3,4,5</sup>, Ryo Iguchi<sup>3</sup>, Pham Van Thach<sup>6,7</sup>, Hiroyuki Awano<sup>6</sup> & Daichi Chiba<sup>1,2,8</sup>

Since the charge current plays a major role in information processing and Joule heating is inevitable in electronic devices, thermal management, i.e., designing heat flows, is required. Here, we report that strain application can change a direction of a heat current generated by magneto-thermoelectric effects. For demonstration, we used metallic magnets in a thin-film form, wherein the anomalous Ettingshausen effect mainly determines the direction of the heat flow. Strain application can alter the magnetization direction owing to the magnetoelastic effect. As a result, the heat current, which is in the direction of the cross product of the charge current and the magnetization vector, can be switched or rotated simply by applying a tensile strain to the metallic magnets. We demonstrate 180° switching and 90° rotation of the heat currents in an in-plane magnetized Ni sample on a rigid sapphire substrate and a perpendicularly magnetized TbFeCo film on a flexible substrate, respectively. An active thermography technique was used to capture the strain-induced change in the heat current direction. The method presented here provides a novel method for controlling thermal energy in electronic devices.

Thermal management is becoming more and more important with the greater miniaturization and performance enhancement of electronic devices. Spin caloritronics<sup>1</sup>, which is a field triggered by observation of the spin Seebeck effect<sup>2</sup>, may help control heat by using spin or magnetization in materials. Among a variety of spin-caloritronic and magneto-thermoelectric phenomena, the spin Peltier effect (SPE)<sup>3–6</sup> and the anomalous Ettingshausen effect (AEE)<sup>7</sup> are candidates for active thermal management. One of their novel points is the controllability of a heat current  $J_q$  with a magnetic field or a magnetization  $M$ . In the AEE,  $J_q$  generated by the charge current  $J_c$  follows the relation  $J_q \propto J_c \times M$ , indicating that the  $J_q$  direction can be rotated or reversed by changing the  $M$  direction. Although the AEE has been known for a long time, such demonstrations and detailed studies have recently been realized by using a lock-in thermography (LIT) technique<sup>4,5,7–13</sup>.

In this paper, we report that mechanically induced strain can switch the direction of the heat currents generated by the magneto-thermoelectric effects through the magnetoelastic coupling. The magnetoelastic effect enables control of the  $M$  direction by using strain instead of using a magnetic field when the strain and/or the magnetostriction constant of the magnetic material are large enough. Previously, a strain of more than 1% was applied to magnetic thin films fabricated on flexible substrates, which resulted in reversible magnetic easy axis switching<sup>14,15</sup>. To demonstrate the strain-induced switching of  $J_q$  induced by the AEE, an in-plane magnetized ferromagnetic Ni film and a perpendicularly magnetized ferrimagnetic TbFeCo thin film deposited respectively on sapphire and flexible polyethylene-naphthalate (PEN) substrates were prepared. In the Ni sample, a 180° reversal of  $J_q$  was observed at an in-plane bias field by bending the sample. In the TbFeCo sample, stretching the PEN substrate could switch the magnetic easy axis from the perpendicular-to-plane to the in-plane direction<sup>14</sup>, resulting

<sup>1</sup>Department of Applied Physics, The University of Tokyo, Bunkyo, Tokyo, 113-8656, Japan. <sup>2</sup>Institute of Scientific and Industrial Research, Osaka University, Ibaraki, Osaka, 567-0047, Japan. <sup>3</sup>National Institute for Materials Science, Tsukuba, 305-0047, Japan. <sup>4</sup>Center for Spintronics Research Network, Tohoku University, Sendai, 980-8577, Japan. <sup>5</sup>Department of Mechanical Engineering, The University of Tokyo, Bunkyo, Tokyo, 113-8656, Japan. <sup>6</sup>Toyota Technological Institute, Nagoya, 468-8511, Japan. <sup>7</sup>Institute of Materials Science, Vietnam Academy of Science and Technology, 18-Hoang Quoc Viet, Hanoi, Vietnam. <sup>8</sup>Center for Spintronics Research Network at Osaka University, Toyonaka, Osaka, 560-6671, Japan. Shinya Ota and Ken-ichi Uchida contributed equally. Correspondence and requests for materials should be addressed to K.U. (email: [UCHIDA.Kenichi@nims.go.jp](mailto:UCHIDA.Kenichi@nims.go.jp)) or D.C. (email: [dchiba@sanken.osaka-u.ac.jp](mailto:dchiba@sanken.osaka-u.ac.jp))

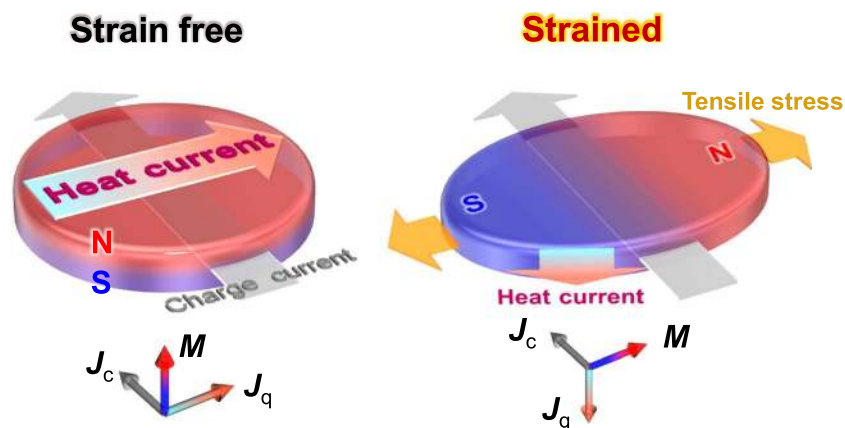


**Figure 1.** Schematic illustration of strain-induced switching of a heat flow. The AEE induced by a charge current  $J_c$  in magnetic materials creates a resultant heat flow  $J_q$ , which is in the direction of the cross product of  $J_c$  and the magnetization  $M$  (see the vector relation for  $J_c$ ,  $J_q$ , and  $M$  shown below the schematics). The direction of  $J_q$  can be switched by stress application because an additional introduced strain can alter the magnetic easy axis (the direction of  $M$ ) through the magnetoelastic effect. The schematic here shows the  $90^\circ$  switching of  $J_q$  induced by the strain-induced rotation of  $M$  from the perpendicular (strain-free) to the in-plane direction (strained).

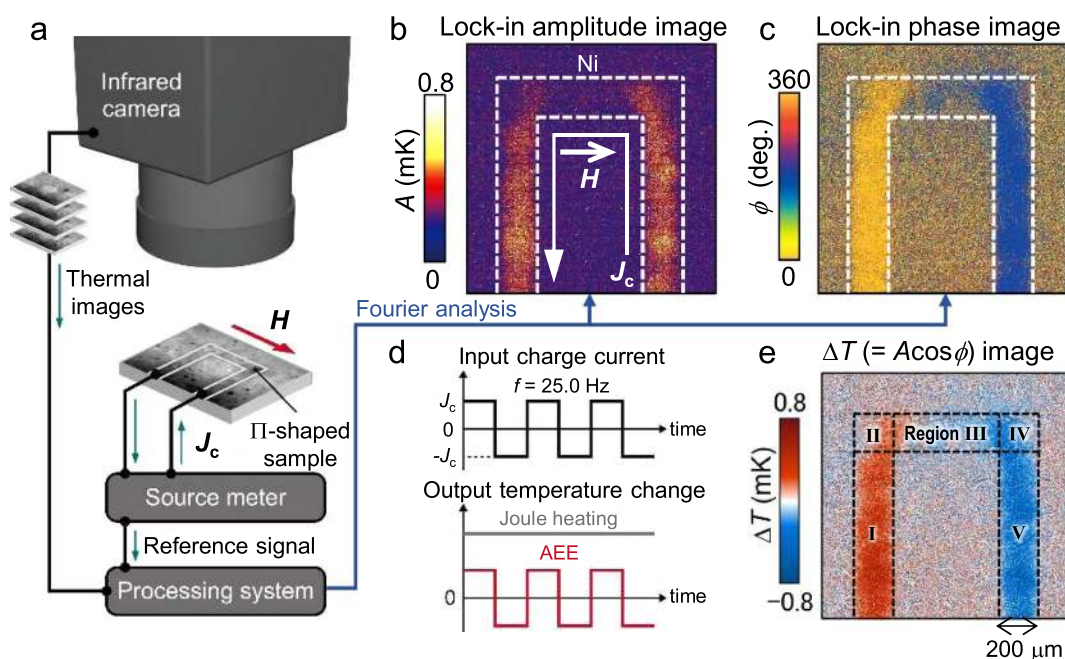


**Figure 2.** Lock-in thermography measurements. (a) A schematic illustration of the LIT system. The temperature modulation synchronized with the output of a source metre is extracted by Fourier analysis through a processing system. (b,c) Images of a lock-in amplitude  $A$  and phase  $\phi$ , respectively. The  $\Pi$ -shaped Ni wire resides in the area surrounded by the dashed lines. (d) Time charts of the input charge current applied to the sample and the expected output, *i.e.*, time-dependent temperature changes induced by the AEE and Joule heating. (e)  $\Delta T (= A \cos \phi)$  image calculated from b and c. The thermal images shown here were taken using the Ni sample at  $\mu_0 H_y = +5.6$  mT without bending the substrate. Regions I–V are defined by the black dashed lines in (e). To enhance the infrared emissivity and ensure uniform emission properties, the surfaces of the samples were coated with insulating black ink, of which the emissivity is  $>95\%$ .

in a  $90^\circ$  rotation of  $J_q$  at zero external magnetic field, as schematically depicted in Fig. 1. This heat-control function may offer an unconventional approach for thermal management technologies.

Temperature modulation due to the AEE-induced  $J_q$  in the samples was detected using the LIT technique at room temperature, as schematically explained in the panels of Fig. 2. For the present experiments, the Ni and TbFeCo films on the substrates were processed into 200- $\mu\text{m}$ -wide  $\Pi$ -shaped wires. An alternating charge current

with a rectangular waveform, zero offset, and a frequency  $f$  of 25 Hz was applied to the wire using a current source metre. Although the Joule heating generated by such an alternating current is constant over time, the temperature modulation due to the AEE oscillates with  $f$ , because the AEE is linearly responsive to the charge current [see Fig. 2d]. Thus, the temperature increase due to Joule heating can be eliminated by extracting the linear response contribution of the temperature modulation via Fourier analysis, enabling pure detection of the AEE. By this LIT measurement, the spatial distributions of the amplitude  $A$  and phase  $\phi$  of the AEE-induced temperature modulation are obtained, where  $\phi$  represents the sign of the temperature modulation depending on the charge current with the time delay due to thermal diffusion. Typical examples of the  $A$  and  $\phi$  images for the Ni sample are shown in Fig. 2b,c, respectively. Figure 2e shows the resultant  $\Delta T (=A\cos\phi)$  image, where  $\Delta T$  is the current-induced temperature modulation with the sign information when the time delay due to thermal diffusion is negligibly small<sup>11</sup>, and this condition can be applied to our experiments.

## Results

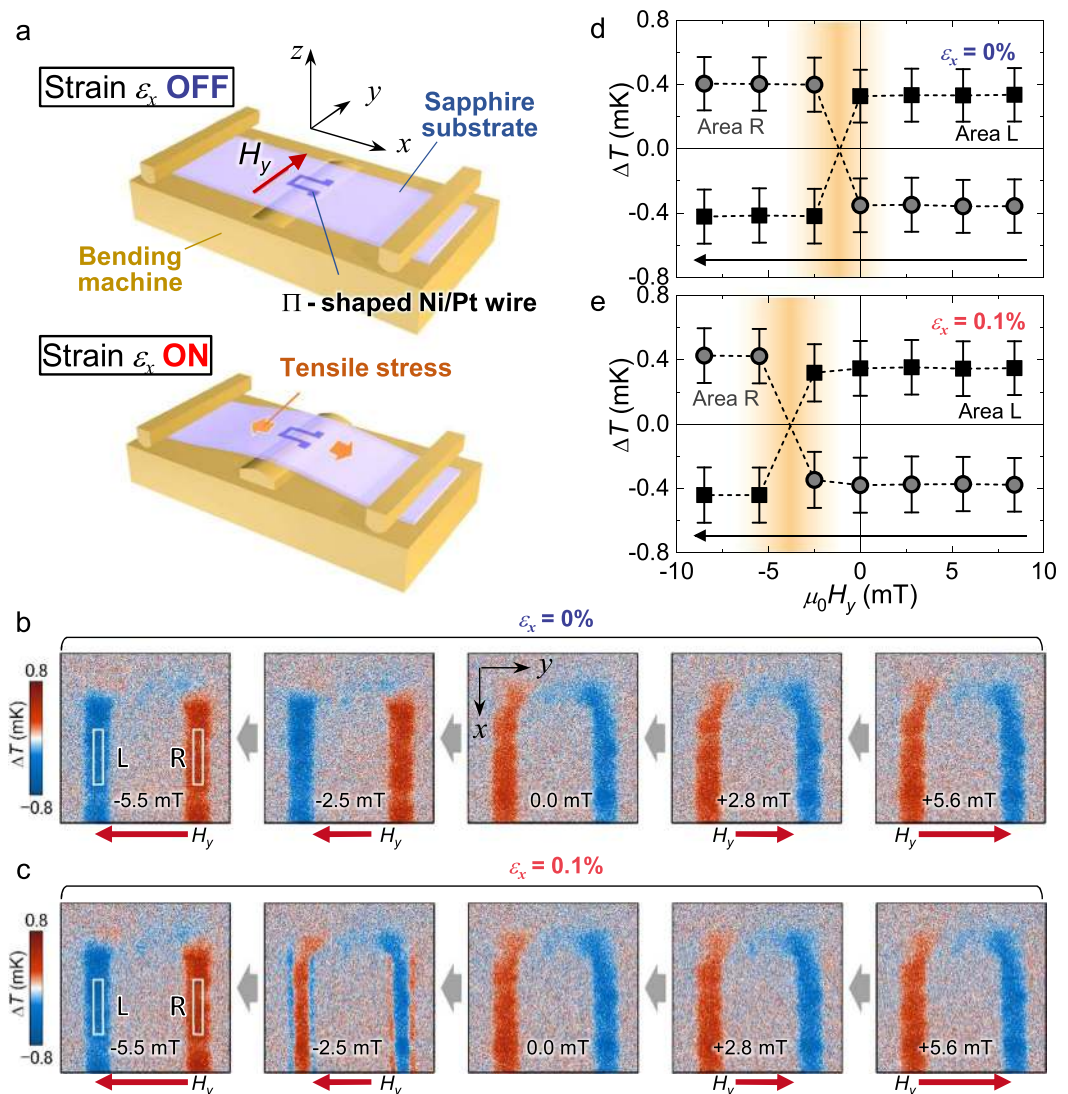
**Strain-induced modulation of heat current switching field.** We firstly show the experimental results of the strain-induced modulation of the 180° switching of the  $J_q$  direction using the in-plane-magnetized Ni sample. Thermal images of this sample were obtained by injecting the alternating charge current with an amplitude  $J_c$  of 10 mA under an applied in-plane magnetic field along the  $y$  axis ( $H_y$ ). A tensile strain  $\varepsilon_x$  was introduced to the Ni film along the  $x$  axis by bending the substrate using a three-point bending machine made of brass [see Fig. 3a and Methods]. The strain applied to the sample surface was calculated using the displacement of the sample centre and the thickness of the substrate. Ni has a negative magnetoelastic constant<sup>15</sup>, *i.e.*, Ni becomes easier to magnetize along the  $y$  axis when the substrate is bent in the present configuration. We note that the initial magnetic anisotropy of regions I and V [see Fig. 2e for a definition of the regions] is along the  $y$  axis because a separate measurement confirms that a  $\mu_0 H_x$  of ~10 mT is needed at  $\varepsilon_x = 0\%$  to completely saturate  $\mathbf{M}$  in these regions toward the  $x$  direction. A tiny built-in strain potentially introduced during sputter-deposition might be attributed to the initial magnetic anisotropy of the sample. In the following discussion, we focus on regions I and V because in the present configuration, the AEE-originated temperature modulation is expected to be seen in these regions, where  $J_c$  ( $\mathbf{M}$ ) is along the  $x$  ( $y$ ) direction<sup>7</sup>.

Figure 3b,c shows the  $\Delta T$  images for  $\varepsilon_x = 0$  and 0.1%. The five images shown as a series of panels were taken by changing  $H_y$  from positive to negative. At any  $H_y$  value, the surface temperature in regions I and V is clearly increased or decreased, indicating that  $J_q$  is along the  $z$  axis. The sign of  $\Delta T$  in these regions was observed to be reversed by reversing the direction of  $J_c$ . This is consistent with the symmetry of the AEE (see Fig. 1). In the negative  $H_y$  region, the sign reversal of  $\Delta T$  occurs in both  $\varepsilon_x = 0$  and 0.1% cases. The reversal is observed in the image at  $\mu_0 H_y = -2.5$  mT for  $\varepsilon_x = 0\%$ , indicating that the coercivity is below 2.5 mT. For the case of  $\varepsilon_x = 0.1\%$ , however,  $\mu_0 H_y = -5.5$  mT is needed for completely switching the sign of  $\Delta T$ . This difference is attributed to the strain-induced enhancement of the coercivity. The direction of  $J_q$  between  $\varepsilon_x = 0$  and 0.1% is opposite at  $\mu_0 H_y = -2.5$  mT, showing that the strain can reverse the  $J_q$  direction by 180°. Note that  $\mathbf{M}$  reversal only at the edge is seen at  $\mu_0 H_y = -2.5$  mT and  $\varepsilon_x = 0.1\%$ . This is most likely due to the weaker magnetic anisotropy because of the smaller thickness at the edge. Figure 3d,e summarises the behaviour of  $\Delta T$  as a function of  $\mu_0 H_y$  for the  $\varepsilon_x = 0$  and 0.1% cases, respectively. In the figures, the averaged  $\Delta T$  values over areas L and R indicated in Fig. 3b,c are plotted, which clearly shows the strain-induced enhancement of the switching field. In region III,  $J_c$  and  $\mathbf{M}$  are expected to be parallel to each other if the magnetic anisotropy is uniform along the whole wire. In fact, the magnitude of  $\Delta T$  for region III is observed to be much smaller than that for regions I and V, consistent with the symmetry of the AEE [see Fig. 3b,c].

**Strain-induced 90° rotation of heat current without an external magnetic field.** Secondly, the 90° switching of  $J_q$  is demonstrated using the perpendicularly magnetized TbFeCo sample. In this experiment, a screw-driven tensile machine made of brass was used to stretch the PEN substrate [Fig. 4b]. In this case, the value of the applied strain  $\varepsilon_x$  was calibrated using the elongation of the sample measured via a microscope and the rotation number of the screw.

Figure 4a shows the results of hysteresis measurements under different strain conditions. The Hall resistance  $R_{\text{Hall}}$ , which is proportional to the  $z$ -component of  $\mathbf{M}$  because of the dominant contribution from the anomalous Hall effect, was measured by sweeping the external magnetic field along the  $z$  direction ( $H_z$ ). A Hall bar-shaped TbFeCo formed on the PEN substrate was used in this experiment (see Methods). As in the case of our previous report<sup>14</sup>, clear easy axis switching from the perpendicular-to-plane direction to the in-plane direction was observed by increasing the strain. A separate experiment confirms that the magnetization easy axis under the strain application is along the  $x$  direction, which is consistent with the positive magnetoelastic constant of TbFeCo<sup>14,16</sup>. By returning the strain to zero, the shape of the hysteresis loop reproducibly returned to a similar shape as that of the initial loop. We note that the remanent magnetization of  $\varepsilon_x = 0\%$  is smaller than the saturation magnetization, which is most likely attributed to the reduced magnetization due to randomly canted spin structures<sup>17</sup>.

Next, the results of the LIT measurement using the II-shaped TbFeCo wire are discussed. In the configuration employed for the present experiment [Fig. 4b], regions I and V are along the  $y$  axis. The  $\Delta T$  images obtained at  $\mu_0 H_z =$  (A)  $-0.15$  T, (B)  $+0.15$  T, and (C)  $0$  T for  $\varepsilon_x = 0, 0.6,$  and  $1.2\%$  are respectively shown in Fig. 4c–e. The LIT images of this sample were obtained by injecting the alternating charge current with  $J_c = 5$  mA.  $H_z$  was changed in the order of A  $\rightarrow$  B  $\rightarrow$  C. Here, the magnetic field-independent background signals were subtracted from the raw LIT images, where the background was calculated from the raw images at  $|\mu_0 H_z| = 0.15$  T and  $\varepsilon_x = 0\%$ . Since the sample has a perpendicular  $\mathbf{M}$  under any  $H_z$  at  $\varepsilon_x = 0\%$ , the AEE-induced  $J_q$  is generated perpendicular to the wire direction. In fact, generation and absorption of heat along the edges of the wire is observed as shown in Fig. 4c, which is consistent with the signal of the AEE with the perpendicularly magnetized configuration<sup>7</sup>. The



**Figure 3.** Strain-induced modulation of a heat current switching field using the Ni sample. (a) A schematic illustration of the experimental setup.  $\varepsilon_x$  was introduced to the Ni film using a three-point bending machine. The electrical connections are omitted from the illustration for simplicity. (b,c)  $\Delta T$  images without bending ( $\varepsilon_x = 0\%$ ) and with bending ( $\varepsilon_x = 0.1\%$ ), respectively. In both measurements,  $\mu_0 H_y$  was reduced from +5.6 mT to -5.5 mT, and the images were taken using the LIT technique at each  $H_y$ . (d,e)  $\Delta T$  as a function of  $\mu_0 H_x$  for the cases of  $\varepsilon_x = 0\%$  and  $0.1\%$ , respectively. The  $\Delta T$  plotted here is the average of the temperature modulation over areas L (square data plots) and R (circle data plots) indicated in b and c. The error bar corresponds to the standard deviation. Although  $180^\circ$  switching of  $J_q$  along the  $z$  axis was observed in both cases, the switching field was different between the two because of the strain-induced enhancement of the coercivity.

direction of heat generation and absorption is opposite for the cases (A,  $-0.15$  T) and (B,  $+0.15$  T) because of the reversed  $M$ . The result for the case (C, 0 T) is almost the same as that for the case (B,  $+0.15$  T) because of the negative remanent  $M$ .

With increasing  $\varepsilon_x$ , the perpendicular magnetic anisotropy of the sample is reduced, and  $M$  points toward the in-plane direction at low  $H_y$ , as shown in Fig. 4a (see the curve for  $\varepsilon_x = 1.2\%$ ). In response to this behavior, the amplitude of the AEE-induced  $\Delta T$  at the wire edges for the case (C, 0 T) decreased with  $\varepsilon_x$ , as observed in the images in Fig. 4c–e. Importantly, the  $\Delta T$  signal at the wire edge disappeared at  $\varepsilon_x = 1.2\%$ , indicating that the in-plane  $J_q$  was almost eliminated. Note that the  $\Delta T$  signal at regions I and V at  $\varepsilon_x = 1.2\%$  is similar to that in the case of the Ni sample. This means that the  $90^\circ$  switching of  $J_q$  from the in-plane to perpendicular direction is realised as a result of the perpendicular to in-plane (along  $x$  axis)  $M$  switching due to the tensile strain. Although a patchy pattern in Fig. 4e reflects randomness of the  $x$ -component of magnetization, the sign of the AEE signals indicate that a substantial portion of magnetization aligns along the  $+x$  direction in the panel C of Fig. 4e, which is possibly due to a small tilt of the magnetic field.



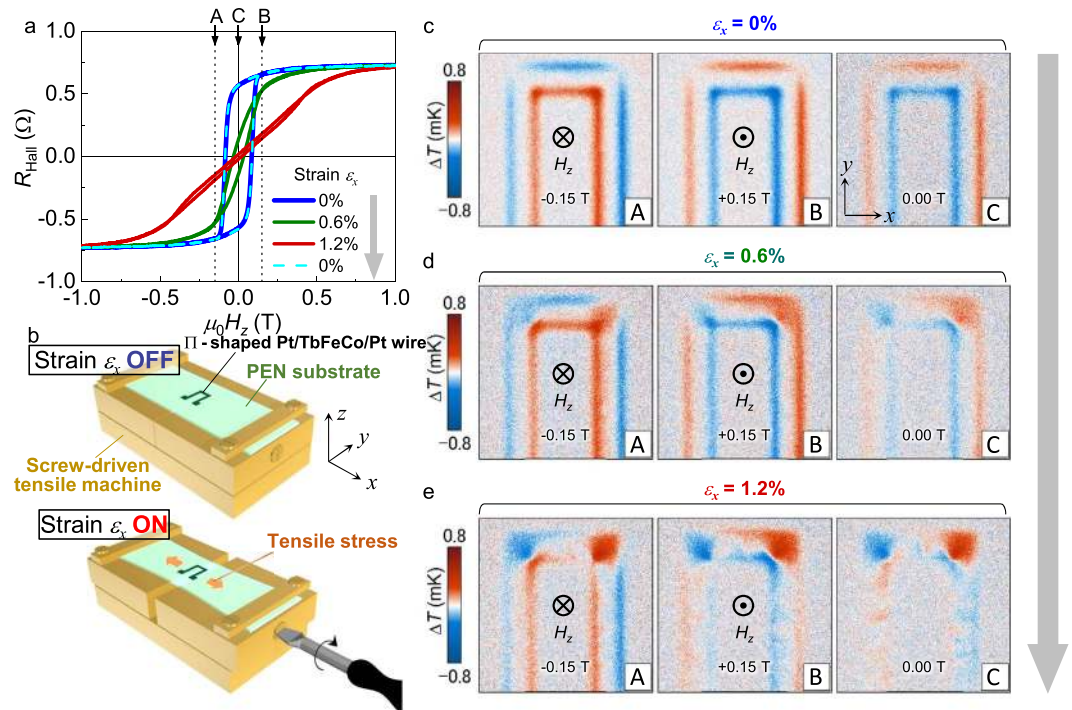


**Figure 4.** Strain-induced 90° switching of a heat current using the TbFeCo sample. (a) The results of the magnetic hysteresis measurement using the anomalous Hall effect.  $H_z$  was swept, and  $R_{\text{Hall}}$  was measured under different in-plane tensile strain conditions. (b) A schematic illustration of the experimental setup for the LIT measurement.  $\varepsilon_x$  was introduced by stretching the substrate. The electrical connections are omitted from the illustration for simplicity. (c–e)  $\Delta T$  images taken under three different  $H_z$  conditions [see dashed lines A–C in a] for  $\varepsilon_x = 0, 0.6,$  and  $1.2\%$ , respectively. Here, the magnetic field-independent background signals were subtracted from the raw LIT images, where the background was calculated from the raw images at  $\mu_0 H_z = \pm 0.15$  T and  $\varepsilon_x = 0\%$ . Complete elimination of the in-plane heat current is realised at  $\varepsilon_x = 1.2\%$  and  $\mu_0 H_z = 0$  T because of the easy axis switching of  $\mathbf{M}$  from the perpendicular to in-plane direction.

## Discussion

Here, we discuss the origin of the observed  $\Delta T$  signals for the Ni and TbFeCo samples. Since both samples have the Pt adjacent layer, which can generate the spin Hall effect-induced spin current<sup>18</sup>, not only the AEE but also the SPE can be a source of the heat current<sup>5,6</sup>. Because of the different symmetries of the AEE and the SPE, the  $\Delta T$  signals in the TbFeCo sample are purely attributed to the AEE if  $\mathbf{M}$  is saturated along the  $z$  axis, while the SPE contribution is eliminated<sup>7</sup>. In contrast, a contribution from the SPE may exist in the Ni and TbFeCo samples in the in-plane magnetized configuration<sup>7</sup>. Nevertheless, the strain-induced control of the heat current demonstrated here is valid, even in the presence of an SPE contribution. To discuss the magnitude of the current-induced temperature modulation in the TbFeCo sample, it is important to recall that  $\Delta T$  is proportional to the length of the ferromagnetic material along the heat current<sup>5</sup>. Since the width of the TbFeCo sample ( $200 \mu\text{m}$ ) is much larger than the thickness ( $6 \text{ nm}$ ), the  $\Delta T$  signal in the perpendicularly magnetized configuration should be several orders of magnitude greater than that in the in-plane magnetized configuration. However, the difference in the  $\Delta T$  magnitude between these configurations is much smaller than this expectation, as shown in Fig. 4e. The possible explanations for this situation are the following: (i) heat loss from the TbFeCo layer to the substrate and black ink (see Methods) reduces the temperature modulation created in the sample plane<sup>7</sup>, and (ii) the lock-in frequency  $f$  dependence of the temperature modulation is different between the two configurations<sup>13</sup>, and the magnitude of the AEE signals in the perpendicularly magnetized configuration decreases with increasing  $f$ , while that in the in-plane magnetized configuration is almost independent of  $f$  (note that all LIT measurements were performed at the high  $f$  value of  $25 \text{ Hz}$ ). Judging from the previously reported studies<sup>7,13</sup>, possibility (i) seems to be the dominant reason. Another important point to be discussed is the difference between the  $\Delta T$  signals of the Ni and TbFeCo samples in the in-plane magnetized configurations. The  $\Delta T$  magnitudes at regions I and V for the latter [Fig. 4e,c] are much smaller than those for the former [Fig. 3b,c]. This result may be attributed to the thin magnetic layer (short length along the heat current<sup>5</sup>), the multi-domain state and the small AEE and/or SPE coefficients in the TbFeCo sample. For further efficient strain control of the heat currents, it is important to look for a material with both high AEE and/or SPE coefficients and good magnetoelastic properties.

We also mention the  $\Delta T$  signals appearing around the corners of the  $\Pi$ -shaped wires, *i.e.*, in regions II and IV. In the TbFeCo sample,  $\Delta T$  clearly appears as the strain is applied. This is consistent with a signal from the anisotropic magneto-Peltier effect (AMPE) when  $\mathbf{M}$  aligns along the  $\pm x$  direction and the sign of the AMPE coefficient is opposite to that of bulk Ni<sup>12</sup>, while the sign of the AEE coefficient is the same as Ni. Although the AMPE should also occur in the Ni sample,  $\Delta T$  is negligibly small compared with the AEE [Fig. 3b,c] because the

high thermal conductivity of the sapphire substrate reduces the magnitude of the AMPE-induced temperature modulation, while the AEE signal in the in-plane magnetized configuration is almost independent of the thermal conductivity of the substrate<sup>13</sup>.

Our experiment demonstrates that the direction of the heat currents due to the spin-caloritronic and/or magneto-thermoelectric phenomena is controlled by a mechanical strain. This suggests that such heat currents can be controlled even by electrical methods, e.g., piezoelectrical control of  $M$ <sup>19,20</sup> and electrical gating-induced magnetic easy axis switching<sup>21,22</sup> or magnetic phase transition<sup>23,24</sup>, though the latter are fundamentally different from the strain-mediated phenomenon. Control of  $M$  using the above methods and the challenges of enhancing  $\Delta T$  may realise a versatile temperature controller or heat current switch, which paves the way for thermal management in increasingly complex electronic and spintronic circuits.

## Methods

**Sample fabrication.** For the Ni sample, a 15-nm-thick Ni film with a 3-nm-thick Pt cap layer was deposited on a 100- $\mu\text{m}$ -thick c-plane sapphire substrate by rf sputtering. By covering the substrate with a metal mask during deposition, a 200- $\mu\text{m}$ -wide  $\Pi$ -shaped wire was formed. For the TbFeCo sample, Pt (4 nm)/Tb<sub>21</sub>Fe<sub>67</sub>Co<sub>12</sub> (6 nm)/Pt (4 nm) layers were deposited on a 50- $\mu\text{m}$ -thick PEN substrate (Q65H, Teijin DuPont) by dc magnetron sputtering. The layers were defined into a  $\Pi$ -shaped wire by photolithography and Ar ion milling.

**Strain machines.** A three-point bending machine made of brass was used for applying strain to the Ni sample. The strain applied to the sample surface was calculated using the displacement of the sample centre and the thickness of the substrate. For the experiment using the TbFeCo sample, a screw-driven tensile machine made of brass was used. In this case, the value of the applied strain was calibrated using the elongation of the sample measured via a microscope and the rotation number of the screw.

**Hall measurement.** The magnetization curves under the tensile strain in the TbFeCo sample shown in Fig. 4a were measured using a Hall bar-shaped TbFeCo with a 30- $\mu\text{m}$ -wide channel, which was fabricated using photolithography and Ar ion milling. A direct current with a magnitude of 100  $\mu\text{A}$  was used to measure  $R_{\text{Hall}}$ .

## References

- Bauer, G. E. W., Saitoh, E. & van Wees, B. J. Spin caloritronics. *Nature Mater.* **11**, 391–399 (2012).
- Uchida, K. *et al.* Observation of the spin Seebeck effect. *Nature* **455**, 778–781 (2008).
- Flipse, J. *et al.* Observation of the spin peltier effect for magnetic insulators. *Phys. Rev. Lett.* **113**, 027601 (2014).
- Daimon, S., Iguchi, R., Hiroki, T., Saitoh, E. & Uchida, K. Thermal imaging of spin Peltier effect Nature Commun. **7**, 13754 (2016).
- Iguchi, R. *et al.* Thermographic measurements of spin-current-induced temperature modulation in metallic bilayers. *Phys. Rev. B* **98**, 014402 (2018).
- Beens, M., Heremans, J. P., Tserkovnyak, Y. & Duine, R. A. Magnons versus electrons in thermal spin transport through metallic interfaces. *J. Phys. D: Appl. Phys.* **51**, 394002 (2018).
- Seki, T., Iguchi, R., Takanashi, K. & Uchida, K. Visualization of anomalous ettingshausen effect in a ferromagnetic film: direct evidence of different symmetry from spin peltier effect. *Appl. Phys. Lett.* **122**, 152403 (2018).
- Straube, H., Wagner, J.-M. & Breitenstein, O. Measurement of the Peltier coefficient of semiconductors by lock-in thermography. *Appl. Phys. Lett.* **95**, 052107 (2009).
- Breitenstein, O., Warta, W. & Langenkamp, M. *Lock-in Thermography: Basics and Use for Evaluating Electronic Devices and Materials* (Springer, 2010).
- Wid, O. *et al.* Investigation of the unidirectional spin heat conveyer effect in a 200 nm thin yttrium iron garnet film. *Sci. Rep.* **6**, 28233 (2016).
- Iguchi, R. & Uchida, K. Charge-current angle and frequency dependences of the spin Peltier effect induced by the spin Hall effect. *Jpn. J. Appl. Phys.* **57**, 0902B6 (2018).
- Uchida, K., Daimon, S., Iguchi, R. & Saitoh, E. Observation of anisotropic magneto-Peltier effect in nickel. *Nature* **558**, 95–99 (2018).
- Das, R., Iguchi, R. & Uchida, K. Systematic investigation of anisotropic magneto-peltier effect and anomalous ettingshausen effect in ni thin films. *Phys. Rev. Applied* **11**, 034022 (2019).
- Ota, S. *et al.* Strain-induced reversible modulation of the magnetic anisotropy in perpendicularly magnetized metals deposited on a flexible substrate. *Appl. Phys. Express* **9**, 043004 (2016).
- Asai, R. *et al.* Stress-induced large anisotropy field modulation in Ni films deposited on a flexible substrate. *J. Appl. Phys.* **120**, 083906 (2016).
- Danh, T. M., Duc, N. H., Thanh, H. N. & Teillet, J. Teillet, Magnetic Mössbauer magnetostrictive studies of amorphous Tb(Fe<sub>0.55</sub>Co<sub>0.45</sub>)<sub>1.5</sub> films. *J. Appl. Phys.* **87**, 7208–7212 (2000).
- Coey, J. M. D. Amorphous magnetic order. *J. Appl. Phys.* **49**, 1646–1652 (1978).
- Kimura, T., Otani, Y., Sato, T., Takahashi, S. & Maekawa, S. Room-temperature reversible spin Hall effect. *Phys. Rev. Lett.* **96**, 156601 (2007).
- Arai, K. I., Muranaka, C. S. & Yamaguchi, M. A new hybrid device using magnetostrictive amorphous films and piezoelectric substrates. *IEEE Trans. Magn.* **30**, 916–918 (1994).
- Novosad, V. *et al.* Novel magnetostrictive memory device. *J. Appl. Phys.* **87**, 6400–6402 (2000).
- Chiba, D. *et al.* Magnetization vector manipulation by electric fields. *Nature* **455**, 515–518 (2008).
- Maruyama, T. *et al.* Large voltage-induced magnetic anisotropy change in a few atomic layers of iron. *Nature Nanotechnol.* **4**, 158–161 (2009).
- Ohno, H. *et al.* *Nature* **408**, 944–946 (2000).
- Chiba, D. *et al.* Electrical control of the ferromagnetic phase transition in cobalt at room temperature. *Nature Mater.* **10**, 853–856 (2011).

## Acknowledgements

The authors thank Tomohiro Koyama, Yuki Hibino, Takahiro Namazu, Taishi Takenobu, and Shimpei Ono for their technical help. S.O. acknowledges the support of the JSPS KAKENHI (Grant No. JP17J03125). K.U. was supported by JST-CREST “Creation of Innovative Core Technologies for Nano-enabled Thermal Management” (Grant No. JPMJCR17I1) and the NEC Corporation. D.C. acknowledges the support of the JSPS KAKENHI (Grant No. JP25220604 and JP19H00860) and Spintronics Research Network of Japan.

### Author Contributions

K.U. and D.C. planned and supervised the study. S.O., P.V.T. and H.A. deposited the Ni and TbFeCo samples. S.O. fabricated the devices. K.U., R.I. and S.O. set up the measurement apparatus. S.O., K.U. and R.I. collected and analyzed the data. K.U. and D.C. produced the figures. S.O., K.U. and D.C. wrote the manuscript. All authors discussed the results.

### Additional Information

**Competing Interests:** The authors declare no competing interests.

**Publisher's note:** Springer Nature remains neutral with regard to jurisdictional claims in published maps and institutional affiliations.



**Open Access** This article is licensed under a Creative Commons Attribution 4.0 International License, which permits use, sharing, adaptation, distribution and reproduction in any medium or format, as long as you give appropriate credit to the original author(s) and the source, provide a link to the Creative Commons license, and indicate if changes were made. The images or other third party material in this article are included in the article's Creative Commons license, unless indicated otherwise in a credit line to the material. If material is not included in the article's Creative Commons license and your intended use is not permitted by statutory regulation or exceeds the permitted use, you will need to obtain permission directly from the copyright holder. To view a copy of this license, visit <http://creativecommons.org/licenses/by/4.0/>.

© The Author(s) 2019